Iron Biomineral Growth from the Initial Nucleation Seed in L-Ferritin

CHEMISTRY
A European Journal

A Journal of
ChemPubSoc Europe

Accepted Article

Title: Iron biomineral growth from the initial nucleation seed in L-ferritin

Authors: Silvia Ciambellotti, Cecilia Pozzi, Stefano Mangani, and Paola Turano

To be cited as: *Chem. Eur. J.* 10.1002/chem.202000064

Link to VoR: http://dx.doi.org/10.1002/chem.202000064

Supported by
ACES

WILEY-VCH

10.1002/chem.202000064

WILEY-VCH

COMMUNICATION

Iron biomineral growth from the initial nucleation seed in L-ferritin

Silvia Ciambellotti,[†[a,b]] Cecilia Pozzi,[†[c]] Stefano Mangani*[c] and Paola Turano*[a,b]

[a] Dr. S. Ciambellotti and Prof. P. Turano
Magnetic Resonance Center (CERM)
University of Florence
Sesto Fiorentino 50019, Italy
E-mail: turano@cerm.unifi.it

[b] Dr. S. Ciambellotti and Prof. P. Turano
Department of Chemistry "Ugo Schiff"
University of Florence
Sesto Fiorentino 50019, Italy

[c] Prof. C. Pozzi and Prof. S. Mangani
Department of Biotechnology, Chemistry and Pharmacy
University of Siena
Siena 53100, Italy
E-mail: stefano.mangani@unisi.it

[†] co-first authors

Supporting information for this article is given via a link at the end of the document

Abstract: X-ray structures of homopolymeric human L-ferritin and horse spleen ferritin were solved by freezing protein crystals at different time intervals after exposure to a ferric salt and revealed the growth of an octa-nuclear iron cluster on the inner surface of the protein cage with a key role played by some glutamate residues. An atomic resolution view of how the cluster formation develops starting from a (μ^3-oxo)tris[(μ^2-glutamato-κO:κO′)](glutamato-κO)(diaquo)triiron(III) seed is provided. The results support the idea that iron biomineralization in ferritin is a process initiating at the level of the protein surface, capable of contributing coordination bonds and electrostatic guidance.

In animals, cytosolic ferritin is a heteropolymer consisting of 24 subunits of H- and L-chains that self-assemble into a hollow structure that hosts iron deposits. L-subunits lack the ferroxidase site for the catalytic oxidation of Fe^{2+}, which is the characteristic feature of H-subunits.[1,2] The H/L ratio in the heteropolymer is determined by the different expression levels of these two components and is tissue and cell specific.[3,4] In humans, cages rich in H subunits are found in tissues requiring fast iron metabolism (e.g, muscles and heart) whereas cages rich in L subunits are found in tissues involved in long-term iron storage (such as liver and spleen). In brain, neurons express mostly H-ferritin, microglia express mostly L-ferritin, oligodendrocytes express similar amounts of both H and L subunits.[5] The H/L ratio determines the rate of iron biomineralization, which occurs as the result of the formation of nano-sized particles of iron oxides within the inner nanocage cavity.[6] From TEM, SAXS, XANES, EELS and SQUID data,[7–10] a polyphasic structure (ferrihydrite, magnetite, hematite) of the bulk biomineral has been proposed, with a ferrihydrite enriched core and a predominantly magnetite-like surface.[7] The amount of L-type subunits influences the morphology, as evidenced by STEM micrographs, giving rise to hollow structures with shapes defined by the number of nucleation sites in the protein shell.[8] Nevertheless, the atomic-level mechanism of the mineral formation remains elusive. Recently, by using time-lapse crystallographic techniques, we have observed biomineral seeds consisting of (μ^3-oxo)tris[(μ^2-peroxo)] triiron(III) clusters at the protein-inner cavity interface that form upon spontaneous oxidation of ferrous ions internalized by recombinant human homopolymeric L-ferritin as well as by natural horse spleen ferritin, which contains about 1-2 H subunits/cage (Fig. S1A and S2A).[11]

Herein, we have modified our experimental setting to extend the observation beyond the formation of these initial nucleation clusters. In the previous experiments, we could observe Fe^{3+} cluster formation via free diffusion of Fe^{2+} through L-ferritin crystals followed by spontaneous oxidation, and flash freezing [11]. Under those experimental conditions, in the homopolymeric L-ferritin the cluster formation was completed after 60 min. Attempts to monitor the growth of the biomineral starting from this initial nucleation seed were frustrated due to a merely technical problem: the oxidation reaction at the crystalline state is slow and when Fe^{2+} aqua-ions, diffusing through the crystal, accumulate above a certain threshold, the crystal quality deteriorates. The underlying idea behind the present experiments is that we might be able to monitor biomineral growth by avoiding the slow oxidation of the Fe^{2+} ions by directly diffusing Fe^{3+} ions. This experimental model could have a functional significance since Fe^{3+} ions produced at the ferroxidase site of H-subunits in the natural heteropolymeric ferritins, also might diffuse towards the nucleation sites of L-subunits to promote biomineral growth.

Crystal structures of HuLf with bound Fe^{3+} ions, were obtained at 15, 30 and 60 minutes of free Fe^{3+} diffusion inside the crystals, followed by flash freezing. After 15 minutes exposure, a (μ^3-oxo) triiron(III) cluster (FeA1, FeA2, FeA3) was observed anchored to the protein surface via Glu60, Glu61 and Glu64 (Fig. 1A and S3A). An oxygen from the carboxylate group of Glu57 binds FeA3. This cluster shows the same arrangement and geometry of ferric ions previously observed in the experiment performed starting from Fe^{2+} (Fig. S1A). The peroxo species bridging the Fe^{3+}, which were produced during the non-catalytic oxidation of Fe^{2+},[11] are missing in the present structure due to the lack of the iron oxidation step.

10.1002/chem.202000064

Exa-coordination of the Fe^{3+} ions is now completed by water/hydroxide molecules. A fourth iron ion, labeled Fe4 in Fig. 1A, interacts with the other carboxylate oxygen of Glu57. Again, a similar arrangement was observed upon Fe^{2+} free diffusion (Fig. S1A). At longer diffusion times (30 min) additional iron ions are found at specific locations nearby the initial seed, suggesting the establishment of clusters of increasing nuclearity, which grow on the inner surface of the ferritin cavity (Fig. 1B-C, S1B and S3B). A main pool of iron ions develops around the initial seed. The octa-iron cluster can be described as composed by three main units (labeled A, B and C): the original (μ^3-oxo)tris (μ^2-glutamato-κO:κO')] triiron(III) unit containing FeA1-3, is flanked on one side by an additional (μ^3-oxo) triiron unit (FeB1-3) anchored to the protein matrix via Glu57; on the other side, two additional iron ions (FeC1-2) bridged one to another by Glu140 and linked to the original (μ^3-oxo)tris(μ^2-glutamato-κO:κO')] triiron(III) via a oxo/hydroxo moiety that connects FeA3, FeC1 and FeC2. The octa-iron cluster is maintained at longer times (60 min) (Fig. 1D and S3C), with some rearrangements of the side chain of Glu57 (now bridging clusters A and B) and a shift in the position of FeC1 and C2. At 90 min of soaking the crystal deteriorates and the process could not be further followed (see Supporting Information). The main structural features of these clusters are summarized in Table S1.

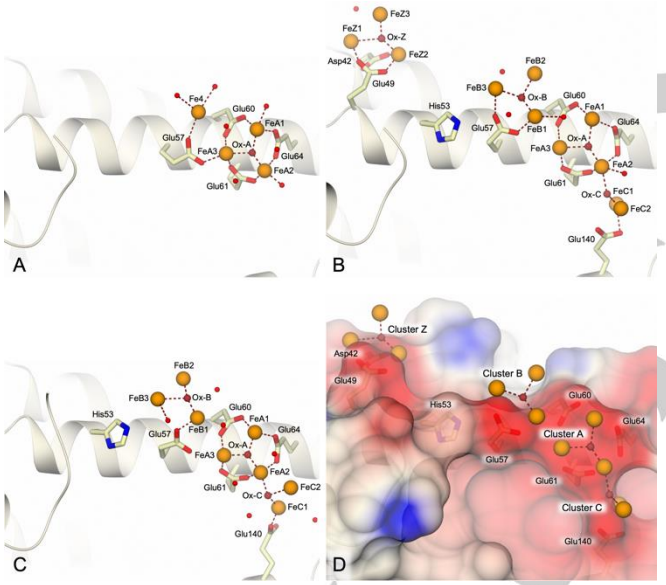

Figure 1. Snapshots of the Fe^{3+} binding events in homopolymeric recombinant human L-ferritin at different times of free Fe^{3+} diffusion in preformed protein crystals (inner cavity view). Binding sites observed after (A) 15 min (PDB id 6TSJ), (B) 30 min (PDB id 6TSA) and (C) 60 min (PDB id 6TSF) of Fe^{3+} exposure. (D) Electrostatic surface representation of the inner cavity of HuLf (calculated on the structure of HuLf after 30 min Fe^{3+} exposure).

A fundamental question at this stage is whether the novel iron ions represent distributed beads interacting with protein sites of lower affinity with respect to the site defined by glutamates 60, 61 and 64, or if a cooperative growth occurs driven by the nucleation site. Substitution of the Glu60, Glu61 and Glu64, which provide the main anchoring points of the (μ^3-oxo)tris[(μ^2-peroxo)] triiron(III) cluster to the protein matrix, with Ala gives rise to a cage variant demonstrated to be unable to form this cluster and with a significantly reduced initial rate of formation of the biomineral.[11]

Here, the crystal structure of the E60AE61AE64A variant shows a single (μ^3-oxo) triiron unit (FeD1-3 in Figures 2C and S4) anchored to the inner cage surface via Glu57 and His53; this species is stably observed at 30 and 60 min (Fig. 2 and S4, Table S2). Therefore, the initial seed seems essential to provide the octa-nuclear species, supporting a cooperative modulation of the biomineral growth alongside the inner cage surface. Nevertheless, this cooperativity seems to be confined to the surface of each subunit, with no ligands/metal ions in common between subunits pairs. However, the octa-nuclear clusters on two-fold symmetry related subunits of the ferritin cage lie at a distance of 8.7 – 9.4 Å (closest distance between symmetry-related iron ions).

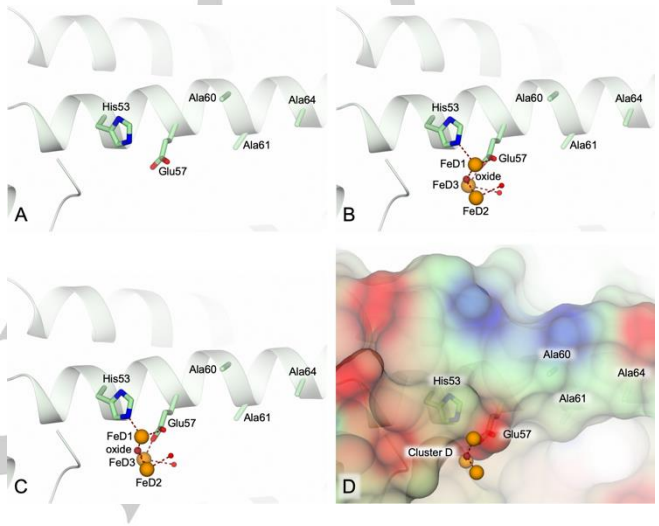

Figure 2. Iron binding events in homopolymeric HuLf E60AE61AE64A variant at different times of free Fe^{3+} diffusion in preformed protein crystals (inner cavity view). Binding sites observed after (A) 15 min (PDB id 6TR9), (B) 30 min (PDB id 6TS0) and (C) 60 min (PDB id 6TS1) of Fe^{3+} exposure. (D) Electrostatic surface representation of the inner cavity of HuLf E60AE61AE64A (calculated on the structure of the triple variant after 30 min Fe^{3+} exposure).

An additional three-nuclear cluster (Z-cluster in Fig. 1B and S3) is transiently observed on the surface of the inner cage of HuLf at a site defined by the residues Asp42 and Glu49. The Z-cluster in the 30 min structure is located at about 9 Å from the octa-iron moiety (the closest iron pair is FeZ2-FeB3 at 9.3 Å). The FeZ1 and FeZ2 ions are close to Asp42 and Glu49 (Table S1) while FeZ3 does not appear to interact with any of the protein residues, but is linked to the other two iron ions via a bridging μ^3-oxo/hydroxo. The Z-cluster is not present in the structure determined after 15 min nor in that at 60 min. The possible functional significance of the Z-cluster, not detected in the previous study based on Fe^{2+} diffusion, was here investigated by mutating the binding protein ligands into Ala and comparing the reaction rates of iron oxidation in solution for the wild type L-ferritin and in its D42AE49A variant. As shown in Fig. 3, by increasing the Fe^{2+}/subunit ratio, the iron oxidation reaction in solution becomes faster thus suggesting that this transient binding site might represent an off-pathway trap. For comparison purposes, the inhibitory effect exerted by the E60AE61AE64A variant is reported.

10.1002/chem.202000064

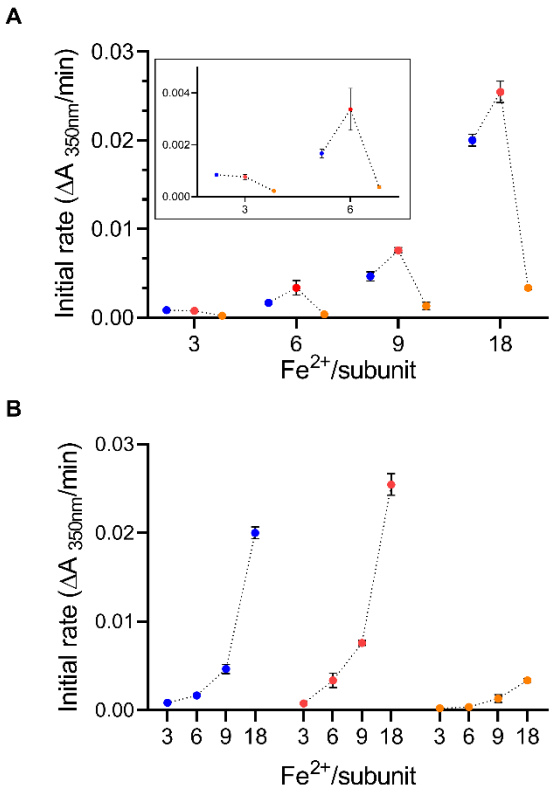

Figure 3. Rate of Fe^{2+} oxidation in WT HuLf (blue symbols) and its D42AE49A (red symbols) and E60AE61AE64A (orange symbols) variants, followed spectrophotometrically as the change in absorbance at 350 nm over time. (A) Direct comparison of the initial rate of the reaction measured in the three ferritin variants as a function of the Fe^{2+}/subunit ratio. The inset shows an enlargement of the values measured at lower concentrations (3Fe^{2+}/subunit and 6 Fe^{2+}/subunit). (B) Trends observed at increasing Fe^{2+}/subunit ratio for each variant. Each point is the mean of three independent experiments with the respective standard deviations. Dotted straight lines connecting experimental points have been added to help visualizing the trend of changes; these lines do not represent any data fitting.

Other Fe^{3+} ions have been detected in HuLf and its triple variant E60AE61AE64A starting from 15 min exposure inside the three-fold channels, which represent the iron entry channels in animal ferritins,[11–16] and on the external protein surface in correspondence of a negative surface area, as detailed in SI.

To ascertain whether the octa-iron cluster formation is a common feature of L-subunits of mammalian ferritins, the Fe^{3+} soaking experiments have been repeated for horse spleen ferritin (HoLf), a commercial heteropolymer with >90% of L subunits,[17] which shares a sequence identity of 87.4 % to HuLf, and maintains all the residues involved in the interaction with the octa-iron cluster. Albeit at lower resolution (Tables S4-S5), the anomalous difference maps show that the structures obtained after 15, 30 and 60 minutes of exposure to Fe^{3+} ions display a similar arrangement of Fe^{3+} ions observed in HuLf at the same time, as reported in Figures 4, S2 and S5, although with some relative rearrangements in the orientation of the bridging carboxylates (Table S3). In particular, Glu60 stably bridges FeA1 and FeB1. Glu57 switches between bridging the FeB1-FeA3 pair and the FeB3-FeB1 pair. The behavior of Glu57 is similar to that observed for HuLf (Fig. S6), although with no correspondence between the specific time points. FeC1 and FeC2 are arranged according to the orientation observed in HuLf at 60 min. The Z-cluster in HoLf is observed at both 30 and 60 min, and sees the involvement of Cys52, modified as S,S-(2-hydroxyethyl)thiocysteine, CME52 (in HuLf, position 52 is taken by a serine, apparently not involved in the cluster binding). These differences might reflect the diversity observed in solution for the reaction kinetics.[18] Consistently with HuLf, HoLf crystals loose diffraction after 60 min exposure.

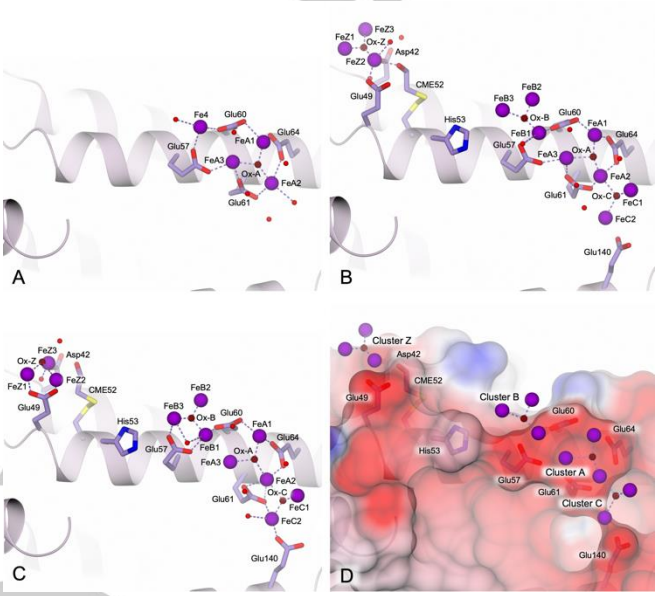

Figure 4. Snapshots of the Fe^{3+} binding events in homopolymeric horse L-ferritin at different times of free Fe^{3+} diffusion in preformed protein crystals (inner cavity view). Binding sites observed after (A) 15 min (PDB id 6TRZ), (B) 30 min (PDB id 6TSX) and (C) 60 min (PDB id 6TSS) of Fe^{3+} exposure. (D) Electrostatic surface representation of the inner cavity of HoLf (calculated on the structure of HoLf after 30 min Fe^{3+} exposure).

In summary, while the bulk biomineral has been detected by HRTEM and XANES, EELS, END, SAXS, the mechanism underlying the initial biomineral formation remained elusive [7–10]. There are examples in the literature suggesting that the growth starts from the inner cage surface.[8] Here we report the first example of high-resolution evidence of this event. While the formation of the tri-nuclear seed is a surface-driven process, the growth from 3 to 8 nuclearity is only indirectly assisted by protein side chains. Overall, iron ions are observed at positions characterized by largely negative surfaces. The continuous negative patch corresponding to the clusters A-C might be designed to assist the initial steps of the biomineralization (Fig. 1D and 4D); this patch is completely cancelled in the variant E60AE61AE64A, where the formation of the octa-iron cluster does not occur. The present observations represent a further proof of the role played by electrostatic guidance in ferritin reactivity.[12,13,19] On the basis of these results, the here observed octa-iron moiety appears as a promising candidate of functional relevance.

Acknowledgements

The authors thank the Diamond Light Source (DLS, Didcot, United Kingdom) and the European Synchrotron Radiation Facility

(ESRF, Grenoble, France) for providing access to the beamlines I03, I04, I04-1, I24 (DLS) and ID29 (ESRF) and all the staff of the synchrotron sources for their assistance in using the beamlines. The authors also thank the staff of the DLS beamline I24 and of the ESRF ID29S Cryobench for their assistance during single-crystal UV/vis absorption microspectrometry analysis. The research leading to these results has been supported by the project CALIPSOplus under the Grant Agreement 730872 from the EU Framework Programme for Research and Innovation HORIZION 2020. We acknowledge Instruct-ERIC, a Landmark ESFRI project, for the support and the use of resources and specifically the CERM/CIRMMP Italy Centre. SC is the recipient of a post-doctoral fellowship co-funded by MIUR-Italy ("Progetto Dipartimenti di Eccellenza 2018-2022" allocated to Department of Chemistry "Ugo Schiff", University of Florence). CP and SM thanks the support of MIUR-Italy "Progetto Dipartimenti di Eccellenza 2018-2022" allocated to Department of Biotechnology, Chemistry and Pharmacy of the University of Siena. The authors thank Prof. S. Torti (University of Connecticut) for providing us with the plasmid encoding wild-type HuLf.

Keywords: L-ferritin • biomineralization • X-ray • metallocluster • nucleation site

[1] R. R. Crichton, J.-P. Declercq, *Biochim. Biophys. Acta.* **2010**, *1800*, 706–718.

[2] J. M. Bradley, G. R. Moore, N. E. Le Brun, *Curr. Opin. Chem. Biol.* **2017**, *37*, 122–128.

[3] P. M. Harrison, P. Arosio, *Biochim. Biophys. Acta.* **1996**, *1275*, 161–203.

[4] P. Arosio, R. Ingrassia, P. Cavadini, *Biochim. Biophys. Acta.* **2009**, *1790*, 589–599.

[5] E. L. MacKenzie, K. Iwasaki, Y. Tsuji, *Antioxid. Redox Signal.* **2008**, *10*, 997–1030.

[6] P. Arosio, F. Carmona, R. Gozzelino, F. Maccarinelli, M. Poli, *Biochem. J.* **2015**, *472*, 1–15.

[7] N. Galvez, B. Fernandez, P. Sanchez, R. Cuesta, M. Ceolin, M. Clemente-Leon, S. Trasobares, M. Lopez-Haro, J. J. Calvino, O. Stephan, et al., *J. Am. Chem. Soc.* **2008**, *130*, 8062–8068.

[8] J. D. López-Castro, J. J. Delgado, J. A. Perez-Omil, N. Gálvez, R. Cuesta, R. K. Watt, J. M. Domínguez-Vera, *Dalton Trans.* **2012**, *41*, 1320–1324.

[9] C. Quintana, J. M. Cowley, C. Marhic, *J. Struct. Biol.* **2004**, *147*, 166–78.

[10] C. Quintana, *Mini Rev. Med. Chem.* **2007**, *7*, 961–75.

[11] C. Pozzi, S. Ciambellotti, C. Bernacchioni, F. Di Pisa, S. Mangani, P. Turano, *Proc. Natl. Acad. Sci. U. S. A.* **2017**, *114*, 2580-2585.

[12] B. Chandramouli, C. Bernacchioni, D. Di Maio, P. Turano, G. Brancato, *J. Biol. Chem.* **2016**, *291*, 25617–25628.

[13] C. Bernacchioni, V. Ghini, E. C. Theil, P. Turano, *RSC Adv.* **2016**, *6*, 21219–21227.

[14] C. Pozzi, F. Di Pisa, C. Bernacchioni, S. Ciambellotti, P. Turano, S. Mangani, *Acta Crystallogr. D Biol. Crystallogr.* **2015**, *71*, 1909–1920.

[15] C. Pozzi, F. Di Pisa, D. Lalli, C. Rosa, E. Theil, P. Turano, S. Mangani, *Acta Crystallogr. D Biol. Crystallogr.* **2015**, *71*, 941–953.

[16] I. Bertini, D. Lalli, S. Mangani, C. Pozzi, C. Rosa, E. C. Theil, P. Turano, *J. Am. Chem. Soc.* **2012**, *134*, 6169–6176.

[17] L. D. Plath, A. Ozdemir, A. A. Aksenov, M. E. Bier, *Anal. Chem.* **2015**, *87*, 8985–8993.

[18] X. Yang, Y. Chen-Barrett, P. Arosio, N. D. Chasteen, *Biochemistry* **1998**, *37*, 9743–9750.

[19] C. Bernacchioni, C. Pozzi, F. Di Pisa, S. Mangani, P. Turano, *Chemistry.* **2016**, *22*, 16213–16219.

10.1002/chem.202000064

WILEY-VCH

COMMUNICATION

Entry for the Table of Contents

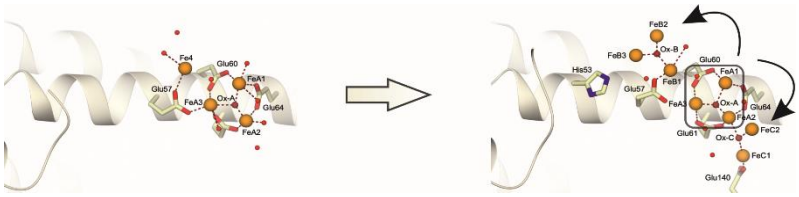

Initial step of ferritin-assisted iron biomineralization: L-type subunits in mammalian ferritins are known to facilitate iron mineralization by providing nucleation sites but the atomic-level mechanism of the mineral formation remains elusive. Time-resolved X-ray crystallography was successfully used to observe iron cluster growth starting from an initial (μ^3-oxo) triiron seed anchored to glutamate residues on the inner ferritin cage.